Sensorless Control of PMSM using DTC Strategy Based on PI-ILC Law and MRAS Observer

Marcel NICOLA[1]
[1]Research Department
National Institute for Research, Development and Testing in Electrical Engineering – ICMET
Craiova, Romania
marcel_nicola@yahoo.com

Claudiu-Ionel NICOLA[1,2], Dumitru SACERDOȚIANU[1]
[2]Department of Automatic Control and Electronics
University of Craiova
Craiova, Romania
claudiu@automation.ucv.ro,
dumitru_sacerdotianu@yahoo.com

***Abstract*—This article presents the sensorless control system of a PMSM (Permanent Magnet Synchronous Motor) based on the DTC (Direct Torque Control) control strategy, where the speed controller is of ILC (Iterative Learning Control) type. This control system is recommended in case of the repetitive tasks performed by the PMSM control system. Also, the superiority of the ILC controller leads to good performance if the load torque (considered as a disturbing signal for the speed control system) has an oscillating variation. In order to increase the reliability of the control system, the speed sensor is replaced with a MRAS (Model Reference Adaptive System) speed observer. The article presents the equations of the PMSM, of the control system, of the observer and the implementation in Matlab/Simulink. The results obtained are presented comparatively for PI, PI-ILC law speed controllers. The superior performance and the parametric robustness are noted for the PI-ILC law speed controller. Based on the results obtained through numerical simulations, the implementation in embedded systems is recommended, in future papers.**

Keywords—State observers; Iterative learning control; Motor drives; Permanenet magnet motors; Automatic control

I. INTRODUCTION

The constructive advantages of PMSM: reduced dimensions, efficient cooling, low harmonic content, losses concentrated in the stator and low inertia were favorable conditions for the study of the PMSM. Among the areas where the PMSM has been used we mention the following: precision electric drives, robotics, computer peripherals and electric vehicles [1-4].

The classic PMSM control systems are FOC (Field Oriented Control) and DTC. Among the modern control structures of the PMSM we mention the adaptive, robust and predictive-type control structures. Among the PMSM intelligent control systems are the fuzzy logic-based systems, genetic algorithms, PSO (Particle Swarm Optimization) algorithms and ANN (Artificial Neural Network)-based algorithms [1-10].

Speed observers are used to increase the reliability of the PMSM control system, thus eliminating the disadvantages of using speed sensors. There are several deterministic estimators: Luenberger, MRAS (Model Reference Adaptive System), SMO (Sliding Mode Observer), but also Kalman-type stochastic estimators. The deterministic observers are characterized by reduced complexity compared to the Kalman-type estimators, which are characterized by high accuracy [11-14].

If the PMSM control structure has repetitive tasks and the load torque has a periodic evolution, it is recommended to use an ILC-type speed controller. Thus, a number of ILC-type controllers have been developed, from the simplest P-ILC law to Global ILC complex controllers [15-19].

This paper presents a PMSM control system based on the DTC-type strategy, where the speed controller is of the PI-ILC-law-type. It presents the superiority of this PI-ILC-law-type control structure over the various PMSM control structures through numerical simulations in Matlab/Simulink, in case of repetitive tasks of the control system. The rest of the paper is structured as follows: Section II describes the mathematical model of the PMSM and the DTC-type control structure. The mathematical model and the implementation structures for the PI-ILC-law-type control law are presented in Section III. Section IV presents the numerical simulations for the PMSM sensorless control system based on the DTC strategy and MRAS-type observer, where the speed controller is of the PI-ILC law type. Conclusions and ideas for the follow-up on the topics referenced in this article are presented in the final section.

II. PMSM AND DTC STRATEGY - MATHEMATICAL MODEL

In the d-q frame, the simplified model of the PMSM is described in equations (1)-(4) [2, 13]. The flux equation is described in (1), the stator voltages equation is described in (2), and the motion equation is described in equation (3) and (4).

$$\begin{bmatrix} \varphi_d \\ \varphi_q \end{bmatrix} = \begin{bmatrix} L_d & 0 \\ 0 & L_q \end{bmatrix} \begin{bmatrix} I_d \\ I_q \end{bmatrix} + \begin{bmatrix} \varphi_0 \\ 0 \end{bmatrix} \quad (1)$$

This paper was developed with funds from the Ministry of Research and Innovation as part of the NUCLEU Program: PN 19 38 01 03.

978-1-7281-6870-8/20/$31.00 ©2020 IEEE

$$\begin{bmatrix} u_d \\ u_q \end{bmatrix} = R_s \begin{bmatrix} I_d \\ I_q \end{bmatrix} + \begin{bmatrix} L_d & 0 \\ 0 & L_q \end{bmatrix} \frac{d}{dt} \begin{bmatrix} I_d \\ I_q \end{bmatrix} + \\ + n_p \omega \begin{bmatrix} 0 & -L_d \\ L_d & 0 \end{bmatrix} \begin{bmatrix} I_d \\ I_q \end{bmatrix} + n_p \omega \begin{bmatrix} 0 \\ \varphi_0 \end{bmatrix} \quad (2)$$

$$T_e = \frac{3}{2} n_p \left((L_d - L_q) I_d I_q + \varphi_0 I_q \right) \quad (3)$$

$$J\dot{\omega} = T_e - T_L - B\omega \quad (4)$$

where: L_d, L_q is the PMSM stator inductances in the d-q reference frame, and R_s is the PMSM stator resistance in the d-q reference frame. According to [2], the simplifications L_d=L_q and R_d=R_q=R_s are accepted.

The rotor velocity is indicated as ω, and the flux linkage as φ_0. Also, the currents and voltages in d-q frame are indicated as I_d, I_q and u_d, u_q. n_p represents the number of pole pairs, and the moment of inertia and the viscous friction coefficient are indicated as J and B.

Fig. 1 presents the classic DTC control structure for the PMSM. The equations in the α-β frame are obtained from the equations in the d-q frame above, by using the inverse Park transform and are presented in equations (5) and (6). As a characteristic of the DTC type strategy, the flux and the torque are directly controlled through simple ON-OFF hysteresis controllers. The flux reference is predefined, and the torque reference is provided by the output of the speed controller [13].

$$\begin{cases} \varphi_\alpha = \int_0^t (u_\alpha - R_s I_\alpha) dt \\ \varphi_\beta = \int_0^t (u_\beta - R_s I_\beta) dt \end{cases} \quad (5)$$

$$\begin{cases} \overline{\varphi}_s = \sqrt{\hat{\varphi}_\alpha^2 + \hat{\varphi}_\beta^2} \\ \angle \hat{\varphi}_s = arctg \dfrac{\hat{\varphi}_\beta}{\hat{\varphi}_\alpha} \end{cases} \quad (6)$$

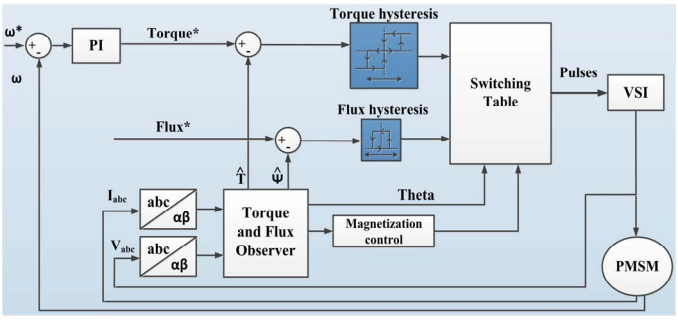

Fig. 1. Block diagram of the DTC strategy for the PMSM

Equations (7) and (8) present the accepted approximations for the torque and the flux to describe the DTC strategy. Thus, by using these approximations for the electromagnetic torque and flux together with angle θ, they represent inputs into the Switching Table. The output of the Switching Table will provide the control pulses for the voltage inverter, which provides the power supply for the PMSM.

$$\overline{\varphi}_s(k+1) \approx \overline{\varphi}_s(k) + \overline{V}_s T_e \rightarrow \Delta\overline{\varphi}_s \approx \overline{V}_s T_e \quad (7)$$

$$T_e = k\left(\overline{\varphi}_s \times \overline{\varphi}_r\right) = k\left|\overline{\varphi}_s\right|\left|\overline{\varphi}_r\right| \sin(\delta) \quad (8)$$

III. PI-ILC CONTROL OF PMSM - MATHEMATICAL MODEL

Fig. 2 presents the simplified mathematical model of the PMSM, described as transfer functions.

Due to the particular context of the application of the ILC-type control, in the block structure in Fig. 2, it can be considered that the transfer function equivalent between i_q^* and i_q (which contains the current control, voltage inverter and the equivalent electrical part of the motor) is equal to 1. The low time constants of these transfer functions in proportion to the mechanical part constants are neglected [2, 14].

The electromagnetic torque T_e is equal to the product between the current i_q and the constant K_e of the torque.

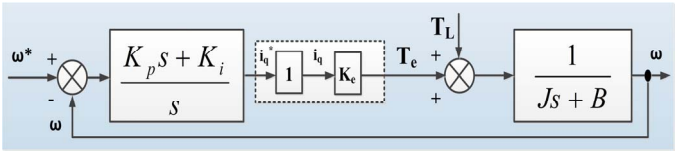

Fig. 2. Block diagram of the transfer function for the PMSM control

In general, if the control system has to perform repetitive tasks, it is necessary to use a special ILC-type controller. The torque T_L represents a disturbance signal for the PMSM control system. Between the regulated output ω and the load torque T_L, the transfer function is expressed in (9), and the equation of the amplitude-frequency characteristic is expressed in (10).

$$H(s) = \frac{\omega(s)}{T_L(s)} = \frac{s}{Js^2 + (B + K_p K_e)s + K_i K_e} \quad (9)$$

$$\left|H(j\omega)\right| = \frac{\omega}{\sqrt{\left(K_i K_e - J\omega^2\right)^2 + \omega^2 (B + K_p K_e)^2}} \quad (10)$$

Based on the equation (4) describing the mathematical model of the PMSM presented in Section II, the following relation can be written:

$$\omega(s) = \frac{T_e(s) - T_L(s)}{Js + B} \quad (11)$$

In Equations (10) and (11) it can be noted that the oscillation frequencies of the torque will be transmitted as oscillation frequencies of the rotor velocity.

Their amplitude can be reduced by increasing K_p, which represents the proportional control factor of the PI-type controller, but by increasing it, a large bandwidth is obtained, which is in contradiction to the requirement to have a stability reserve of the system. It results that the PI controller can reduce the disturbances in limited mode. Therefore, if the control system of the PMSM has repetitive tasks, values of the control from the previous cycle and values of the system output error can be used so that the control generated in the next iteration cycle is generated based on the "iterative learning law".

In the case of the "iterative learning law" of the form (P-ILC law):

$$u_{k+1}(t) = \alpha u_k(t) + \phi e_{k+1}(t) \tag{12}$$

where: $u_j(t)$ is the control signal, $e_j(t)$ is the output error of the system; k is the iteration number, ϕ is the learning factor. Usually ϕ can be selected as equal to K_p (proportional control factor). The necessary and sufficient condition for convergence is that the factor α meets the condition $|\alpha|<1$.

Under these conditions where the type of controller is PI-ILC law (see Fig. 3), the transfer function expressed by equation (9) becomes:

$$H(s) = \frac{\omega(s)}{T_L(s)} = \frac{1-\alpha e^{-\tau s}}{(Js+B)(1-\alpha e^{-\tau s}) + K_e\phi} \tag{13}$$

For $\tau=2\pi/\omega_e$, where ω_e is the speed of the electric angle $\omega_e=n_p\omega$, a rejection of the exogenous signal occurs (with the frequency $n\omega_e$, where n is a positive integer):

$$e^{-\tau s} = e^{-je\omega\tau} = e^{-j2n\pi} = 1 \tag{14}$$

The PI-ILC law discrete control becomes:

$$u^*_{q,k+1}(z) = \alpha u^*_{q,k}(z) + \phi e_{k+1}(z) \tag{15}$$

For $N=\tau/T_s$, where T_s is the sampling period can be obtained based on equation (15):

$$z^{-N} u^*_{q,k+1}(z) = u^*_{q,k}(z) \tag{16}$$

With these, the transfer function in z domain of the PI-ILC law control becomes:

$$G(z) = \frac{u^*_{q,k+1}(z)}{e_{k+1}(z)} = \frac{\phi z^N}{z^N - \alpha} \tag{17}$$

The $|\alpha|<1$ condition ensures the stability of the controller.

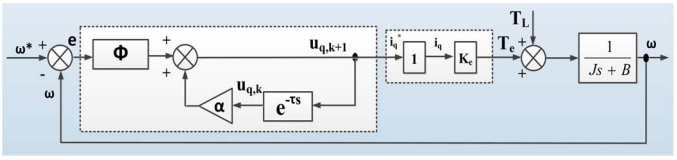

Fig. 3. Block diagram of the transfer function for the ILC law control of the PMSM

Superior performance is achieved by using a PI-ILC-law-type control law for the PMSM control [17].

$$u_{q,k+1} = \alpha u_{q,k} + \Phi e_{k+1} + \Gamma \int e_{k+1} dt \tag{18}$$

where: α represents the learning factor, Φ and Γ are the learning gain (see Fig. 4).

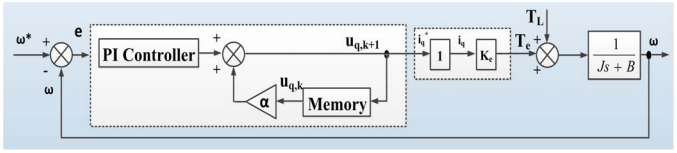

Fig. 4. Block diagram of the transfer function for the PI-ILC law control of the PMSM

Usually $\Phi=K_p$ and $\Gamma=K_i$, can be selected, where K_p is the proportional control factor and K_i is the integration factor of the PI controller. The output of the PI-ILC law noted $u_{q,k+1}$ represents the i_q reference.

By considering W(s) as the transfer function of the mechanical part, the following relation can be written:

$$G(s) = K_e W(s) \tag{19}$$

Thus, the following relation is obtained in the time domain:

$$\omega_{k+1} = g u_{q,k+1} \tag{20}$$

The error of the control system is expressed by:

$$e_{k+1} = \omega^* - \omega_{k+1} = \omega^* - g u_{q,k+1} \tag{21}$$

Based on the above relations, the error equation can be written as follows:

$$e_{k+1} = \alpha e_k - g\left(K_p e_{k+1} + K_i \int e_{k+1} dt\right) + (1-\alpha)\omega^* \tag{22}$$

Thus the following estimate is obtained:

$$\left\| e_{k+1} \right\|_\infty = \max_{0 \le t \le T} \left(\alpha e_k - g\left(K_p e_{k+1} + K_i \int e_{k+1} dt\right) + (1-\alpha)\omega^*\right) \tag{23}$$

Thus the condition for convergence for the PI-ILC controller becomes:

$$\frac{|\alpha|}{|1 - gK_p - gK_i t|} \le 1 \tag{24}$$

The tuning of the parameters of the PI-ILC controller (α, K_p, K_i) is done by observing the inequality (24).

IV. Sensorless Control of the PMSM Using ILC and DTC Strategy – Numerical Simulation

Fig. 5 presents the block diagram for the implementation in Matlab/Simulink of the PMSM control system whose main purpose is the minimization of the torque and rotor speed ripple under the situations where the PMSM tasks and exogenous disturbances are repetitive. In this respect, the DTC strategy is used, but the controller in the outer speed control loop is of the PI-ILC law type. The output of this controller represents the reference for the torque control loop. Also, the control is of the sensorless type, therefore the speed sensor will be replaced with a MRAS speed observer.

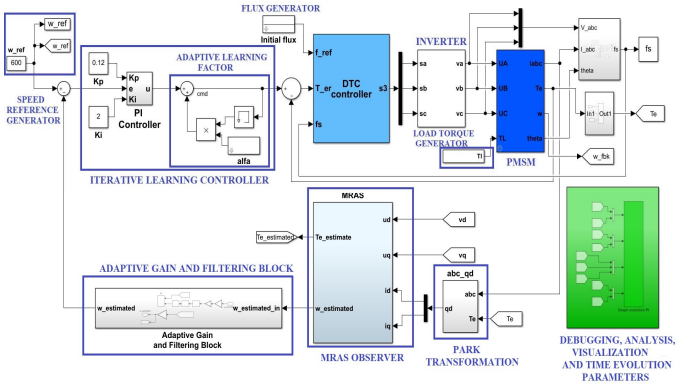

Fig. 5. Rotor speed and stator resistance estimation scheme for MRAS

To achieve the sensorless control, it is necessary to estimate the rotor velocity. Also, equation (5) shows the necessity to estimate the stator resistance. For these, an MRAS observer will be used; its operating principle is based on comparing the outputs of two systems. The first one is called a reference model, and the second one is an adaptive model, whose operating equations depend on the estimated parameters, and thus adjusts continuously. The error between the outputs of these two systems undergoes the process of an adaptation mechanism that will provide the output estimated parameters (see Fig. 6). The reference model of the MRAS observer is derived from equation (2). It represents the actual mathematical model of the PMSM and is described as follows:

$$\dot{x} = Ax + BU + C \tag{25}$$

where: $x = \begin{bmatrix} I_d & I_q \end{bmatrix}^T$, $U = \begin{bmatrix} u_d & u_q \end{bmatrix}^T$, $A = \begin{bmatrix} -\frac{R_s}{L_d} & n_p\omega \\ -n_p\omega & -\frac{R_s}{L_d} \end{bmatrix}$,

$B = \frac{1}{L_d}\begin{bmatrix} 1 & 0 \\ 0 & 1 \end{bmatrix}$, $C = \begin{bmatrix} 0 \\ -\frac{\varphi_0}{L_d} n_p \omega \end{bmatrix}$.

The adaptive model is similar to the reference model, and it is defined by the following relations:

$$\dot{\hat{x}} = \hat{A}\hat{x} + BU + \hat{C} \tag{26}$$

where: $\hat{x} = \begin{bmatrix} \hat{I}_d & \hat{I}_q \end{bmatrix}^T$, $U = \begin{bmatrix} u_d & u_q \end{bmatrix}^T$, $\hat{A} = \begin{bmatrix} -\frac{\hat{R}_s}{L_d} & n_p\hat{\omega} \\ -n_p\hat{\omega} & -\frac{\hat{R}_s}{L_d} \end{bmatrix}$,

$B = \frac{1}{L_d}\begin{bmatrix} 1 & 0 \\ 0 & 1 \end{bmatrix}$, $\hat{C} = \begin{bmatrix} 0 \\ -\frac{\varphi_0}{L_d} n_p \hat{\omega} \end{bmatrix}$.

To demonstrate the stability of the MRAS observer, the system of errors is defined as follows:

$$\dot{\bar{e}} = \dot{x} - \dot{\hat{x}} = A\bar{e} + \left(A - \hat{A}\right)\hat{x} + C - \hat{C} = Ae + W \tag{27}$$

where: $W = \left(A - \hat{A}\right)\hat{x} + \begin{bmatrix} 0 \\ -\frac{\varphi_0}{L_d} n_p \end{bmatrix}(\omega - \hat{\omega})$.

The asymptotic stability of the MRAS observer is demonstrated by means of Popov's stability theory (hyperstability theory) [3, 13]. Thus, the structure of the closed-loop observer contains in the direct path the strictly positive real transfer function $H(s)=(sI-A)^{-1}$, and the feedback is provided by the adaptation mechanism. These can be synthesized by fulfilling the following condition:

$$\int_0^{t_0} \bar{e}^T W dt \ge -\gamma^2 \tag{28}$$

where: γ is a finite positive real constant, and $t_0 \ge 0$.

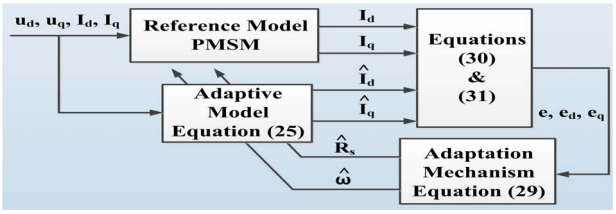

Fig. 6. Rotor speed and stator resistance estimation scheme for MRAS

The adaptation mechanism for the stator resistance and rotor speed presented in Fig. 7 is defined by the following relations:

$$\begin{cases} \hat{R}_s = \frac{1}{L_d}\int_0^t \left(e_d\hat{I}_d + e_q\hat{I}_q\right)dt \\ \hat{\omega} = \frac{1}{n_p}\left(k_p e + k_i\int_0^t e dt\right) \end{cases} \tag{29}$$

$$e = I_d \hat{I}_d - I_q \hat{I}_q - \frac{\varphi_0}{L_d} e_q \tag{30}$$

$$e_d = I_d - \hat{I}_d; \quad e_q = I_q - \hat{I}_q \tag{31}$$

where: k_p and k_i represent the proportional and integral constants of the PI controller.

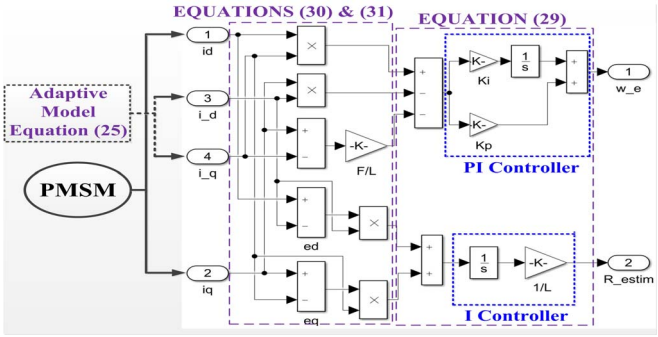

Fig. 7. Block diagram for Simulink implementation of MRAS observer

The results of the numerical simulations performed in Matlab/Simulink for the estimation of the rotor speed of a PMSM with the nominal parameters indicated in Table I are presented in Fig. 8.

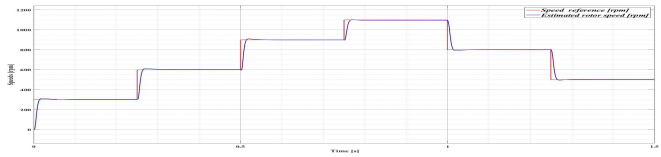

Fig. 8. Time evolution of the rotor speed estimation from the MRAS observer

For the numerical simulation in the Matlab/Simulink environment, a PMSM with the nominal parameters given in Table I was selected.

TABLE I. PMSM - NOMINAL PARAMETERS

Parameter	Value	Unit
Stator resistance - R_s	2.875	Ω
q and d inductance - L_q and L_d	0.0085	H
Combined inertia of rotor and load - J	0.8e-3	kg·m^2
Combined viscous friction of rotor and load - B	0.005	N·m·s/rad
Flux induced by the permanent magnets of the rotor in the stator phases - λ_0	0.175	Wb
Pole pairs number - P	4	-

For a reference speed profile: [0 0.25 0.5 1]s →[300 600 900 600]rpm and a load torque profile, with low/medium variation, described by the sequence: [0 0.25 0.5 0.75 1.25] s → [1 2 3 3 2] Nm, the results of the simulation of the DTC-type control system of the PMSM with the parameters described in Table I, are presented in Fig. 9. A good response of the control system is noted. If the tasks of the DTC-strategy-based control system of the PMSM are repetitive and the load torque has a periodic shape, the PI speed controller cannot eliminate the ripple in the speed response. For a torque variation of 1+sin((2*pi*t)/0.15), the response of the DTC-type control system with PI controller is presented in Fig. 10, where it is noted that in stationary regime the amplitude of rotor speed oscillations is of 8rpm.

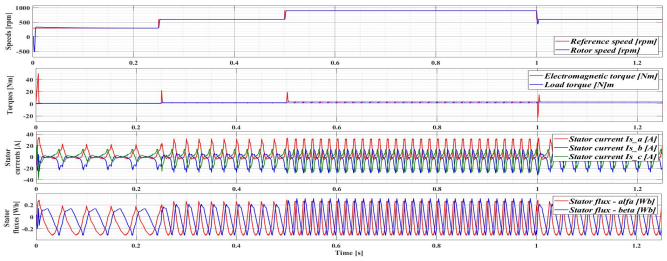

Fig. 9. Simulation of the PMSM time evolution with DTC strategy and speed PI controller

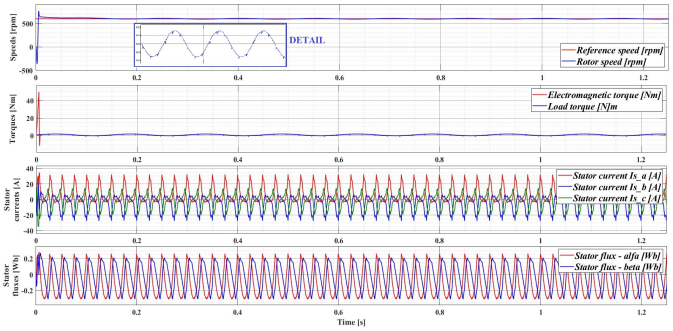

Fig. 10. Simulation of the PMSM time evolution with DTC strategy and speed PI controller and oscillating load torque

By using the P-ILC law type control, an improved response is obtained regarding the speed response ripple (4rpm), but the transitory regime has an overshooting, and the response time is increased, as compared to the case when the DTC strategy and the PI speed controller are used (see Fig. 11). Superior performance can be obtained when using a PI-ILC law control (see Fig. 12). A good transitory regime is noted, and in stationary regime the amplitude of the rotor speed oscillations is of 1.5rpm. Also, the control system has good parametric robustness, given that for a 50% increase of the inertia factor J, the response of the system presented in Fig. 13 does not show qualitative changes, as compared to the case where J has a nominal value.

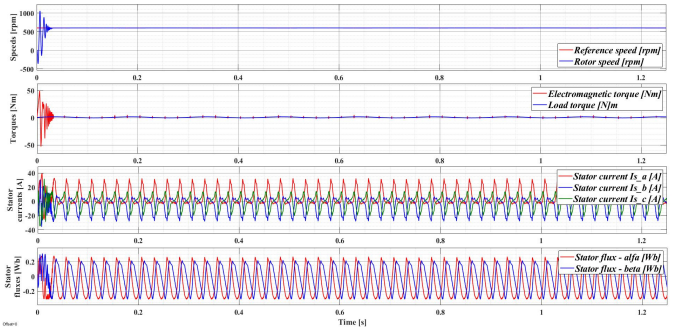

Fig. 11. Simulation of the PMSM time evolution with DTC strategy and P-ILC law and oscillating load torque

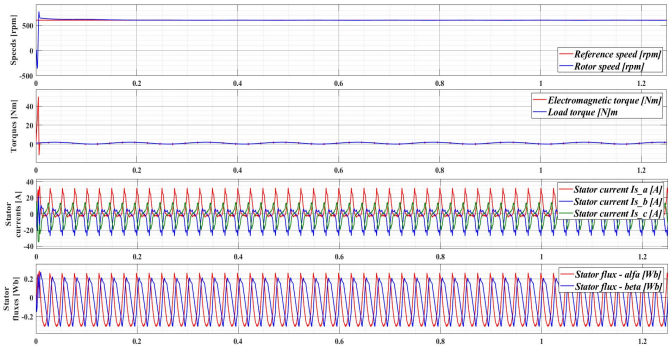

Fig. 12. Simulation of the PMSM time evolution with FOC strategy and PI-ILC law and oscillating load torque

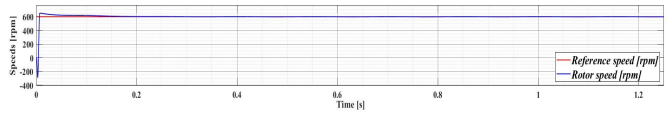

Fig. 13. Simulation of the PMSM time evolution with DTC strategy and PI-ILC law, oscilant load torque and 50% increase of J parameter

The ripple of the speed signal is defined as [5]:

$$\omega_{rip} = \sqrt{\frac{1}{N}\sum_{i=1}^{N}\left(\omega(i) - \omega_{ref}(i)\right)^2} \tag{32}$$

where: N is the number of samples, ω and ω_{ref} are the rotor speed and the prescribed reference of speed, respectively. A ω_{rip} value of 38.21rpm is obtained for the PI speed controller and a 25% reduction of this value for the PI-ILC law speed controller.

V. CONCLUSIONS

This article presents the sensorless control system of a PMSM based on the DTC control strategy, where the speed controller is of PI-ILC type. This type of control is applied with very good results to minimize the speed signal ripple if the PMSM control system performs repetitive tasks, and the load torque is oscillating. In order to increase the reliability of the control system, the speed sensor is replaced with a MRAS-type speed observer. The article presents the equations of the PMSM, of the control system, of the observer and the implementation in Matlab/Simulink. The results obtained are presented comparatively for a PI, PI-ILC law speed controller. The superior performance and the parametric robustness are noted for the PI-ILC law speed controller. Based on the results obtained through numerical simulations, the implementation in embedded systems is recommended, in future papers.

REFERENCES

[1] V. Utkin, J. Guldner, J. Shi, Sliding mode control in electromechanical systems, second edition. Automation and Control Engineering, Taylor & Francis, 2009.

[2] B. K. Bose, Modern power electronics and AC drives, Prentice Hall, Knoxville, Tennessee, USA, 2002.

[3] Y. Zhao, "Position/speed sensorless control for permanent-magnet synchronous machines," Ph.D. dissertation, Electrical Engineering, Univ. Nebraska – Lincoln, Lincoln, 2014.

[4] Z. Tan and X. Gao, "A Review of State-of-the-art Control and Optimization Methods in Permanent Magnet Synchronous Machine Drives," *IEEE 17th International Conference on Industrial Informatics (INDIN)*, Helsinki, Finland, 2019, pp. 611-616.

[5] B. Ning, S. Cheng, and Y. Qin, "Direct torque control of PMSM using sliding mode backstepping control with extended state observer," in Journal of Vibration and Control , vol. 24, no.4, pp. 694-707, Feb. 2018.

[6] M. Yuhendri, A. Ahyanuardi, A. Aswardi, "Direct Torque Control Strategy of PMSM Employing Ultra Sparse Matrix Converter," in International Journal of Power Electronics and Drive System (IJPEDS), vol. 9, no. 1, pp. 64-72, March 2018.

[7] M. Nicola and C. Nicola, "Sensorless Control for PMSM Using Model Reference Adaptive Control and back-EMF Sliding Mode Observer," *International Conference on Electromechanical and Energy Systems (SIELMEN)*, Craiova, Romania, 2019, pp. 1-7.

[8] B. Islam, A. Aissa, K. Katia, and S. Hocine, "Predictive Direct Torque Control Based on New Formulation and Fuzzy Logic for Permanent Magnet Synchronous Machine," *International Conference on Electrical Sciences and Technologies in Maghreb (CISTEM)*, Algiers, Algeria, 2018, pp. 1-6.

[9] S. Lu and X. Wang, "Observer-Based Command Filtered Adaptive Neural Network Tracking Control for Fractional-Order Chaotic PMSM," in IEEE Access, vol. 7, pp. 88777-88788, July 2019.

[10] M. Mutluer and O. Bilgin, "Design optimization of PMSM by particle swarm optimization and genetic algorithm," *12 International Symposium on Innovations in Intelligent Systems and Applications*, Trabzon, Turkey, 2012, pp. 1-4.

[11] K. Kyslan, V. Šlapák, V. Fedák, F. Ďurovský, and K. Horváth, "Design of load torque and mechanical speed estimator of PMSM with unscented Kalman filter - An engineering guide," *19th International Conference on Electrical Drives and Power Electronics (EDPE)*, Dubrovnik, Croatia, 2017, pp. 297-302.

[12] N. Henwood, J. Malaizé, and L. Praly, "A robust nonlinear Luenberger observer for the sensorless control of SM-PMSM: Rotor position and magnets flux estimation," *38th Annual Conference on IEEE Industrial Electronics Society (IECON)*, Montreal, Canada 2012, pp. 1625-1630.

[13] A. Aissa, K. Ameur, and B. Mokhtari, "MRAS for Speed Sensorless Direct Torque Control of a PMSM Drive Based on PI Fuzzy Logic and Stator Resistance Estimator," in Transaction on Control and Mechanical Systems, vol. 2, no. 7, pp. 321-326, Jul. 2013.

[14] X. Zhang, "Discussion on "Torque Ripple Minimization of PMSM Based on Robust ILC via Adaptive Sliding Mode Control"," in *IEEE Access*, vol. 7, pp. 94899-94906, 2019.

[15] Q. Fei, Y. Deng, H. Li, J. Liu and M. Shao, "Speed Ripple Minimization of Permanent Magnet Synchronous Motor Based on Model Predictive and Iterative Learning Controls," in *IEEE Access*, vol. 7, pp. 31791-31800, 2019.

[16] J. Liu, H. Li, and Y. Deng, "Torque Ripple Minimization of PMSM Based on Robust ILC Via Adaptive Sliding Mode Control," in IEEE Transactions on Power Electronics, vol. 33, no. 4, pp. 3655-3671, April 2018.

[17] L. Wenshan, Z. Jian, and L. Yong, "A simpler and more efficient iterative learning controller for PMSM torque ripple reduction," *International Conference on Electrical Machines and Systems (ICEMS)*, Busan, South Korea, 2013, pp. 1231-1235.

[18] C. Xia, W. Deng, T. Shi, and Y. Yan, "Torque Ripple Minimization of PMSM Using Parameter Optimization Based Iterative Learning Control," in Journal of Electrical Engineering and Technology, vol. 11, no. 2, pp. 425-436, March 2016.

[19] S. Mandra, K. Galkowski, E. Rogers, A. Rauh, and H. Aschemann, "Performance-Enhanced Robust Iterative Learning Control With Experimental Application to PMSM Position Tracking," in IEEE Transactions on Control Systems Technology, vol. 27, no. 4, pp. 1813-1819, July 2019.